Barrier Cavities in the Brookhaven AGS

BNL/SNS TECHNICAL NOTE

NO. 063

M. Blaskiewicz, J. M. Brennan, T. Roser, K. Smith, R. Spitz, A. Zaltsman (BNL)
M.Fujieda, Y. Iwashita, A. Noda (Kyoto U.)
M. Yoshii (KEK, Tsukuba)
Y. Mori, C. Ohmori, Y. Sato (KEK, Tanashi)

May 20, 1999

ALTERNATING GRADIENT SYNCHROTRON DEPARTMENT
BROOKHAVEN NATIONAL LABORATORY
UPTON, NEW YORK 11973

BARRIER CAVITIES IN THE BROOKHAVEN AGS*

M. Blaskiewicz†, J.M. Brennan, T. Roser, K. Smith,
R. Spitz, A. Zaltsman, BNL, Upton, NY 11973, USA
M. Fujieda, Y. Iwashita, A. Noda, Kyoto University, Gokanosho, Uji,Kyoto 611, JP
M. Yoshii, KEK, 1-1 Oho, Tsukuba 305, JP
Y. Mori, C. Ohmori, Y. Sato, KEK - Tanashi, Tanashi 188, JP

Abstract

In collaboration with KEK two barrier cavities, each generating 40 kV per turn have been installed in the Brookhaven AGS. Machine studies are described and their implications for high intensity operations are discussed.

1 INTRODUCTION

During the 1998 high energy physics run the rf system in the AGS Booster ran with harmonic number $h = 1$, and the AGS ran with $h = 6$. This allowed for six Booster transfers per AGS cycle, even though the machine circumferences are in the ratio 1:4. Running the Booster with $h = 1$ opened up the possibility of emittance conserving barrier bucket manipulations using two dedicated barrier cavities. The controls were set up to allow barrier cavity operation in a "pulse stealing" mode wherein the machine settings for the production cycle were changed to those appropriate for barrier operations for a few machine cycles and then switched back to the production cycle settings. This allowed for machine studies and hardware development over the entire run.

The principles of barrier cavity operation have been described elsewhere[1, 2, 3]. This paper focuses on hardware configurations and conclusions.

2 EXPERIMENTAL SETUP

The cavity and amplifier parameters are summarized in Table 1. As is clear from the table the two devices are quite different. The large R/Q of the cavity supplied by KEK allows the use of a small amplifier but requires beam loading compensation at moderate beam currents. The feedforward system is broad band with a full turn of delay[4]. The voltage waveforms without beam, corrected for uncompensated capacitive dividers, are shown in Figure 1. Dynamical implications are considered next.

Let T_0 and E_0 be the revolution period, and synchronous energy, respectively. Denote the arrival time of a proton as $nT_0 + \tau$ on the nth turn and let $\delta = E - E_0$ be its relative energy deviation. The proton equations of motion

Table 1: Cavity parameters

Parameter	BNL cavity	KEK cavity
core material	ferrite	Finemet[1]
gaps per cavity	4	4
$f_{\rm res}$	2.6MHz	1.1MHz
R/Q per gap	180Ω	1500Ω
Q	30	0.6
coupling	single ended	push-pull
amplifier rating	600kW	30kW each
beam loading correction	none	feed-forward

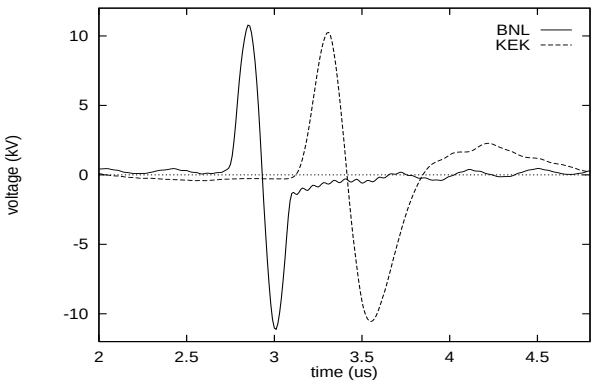

Figure 1: Gap voltage without beam over one AGS revolution period.

are derivable from the Hamiltonian

$$H(\tau,\delta) = \frac{\eta\delta^2}{2\beta^2 E_0} - q f_0 \int_0^\tau V(t')dt', \qquad (1)$$

where η is the frequency slip factor, $\beta = v/c$, q is the proton charge, and f_0 is the revolution frequency. The equations of motion are $d\tau/dt = \partial H/\partial\delta$ and $d\delta/dt = -\partial H/\partial\tau$. The integral of the voltage waveform is proportional to the longitudinal potential well and the familiar pictures of introductory mechanics are applicable.

The voltage integrals without beam are shown in Figure 2. Protons are repelled from high potential regions and undergo stable oscillations in low potential regions. Measurements were made using low intensity small emittance injected bunches to map out the potential wells. It was found that potential in the off-pulse region of the BNL cavity is flatter than show in the figure, which is consistent with the

* Work supported by US Department of Energy
† Email: mmb@bnl.gov
[1] Trademark, Hitachi Metals, Ltd.

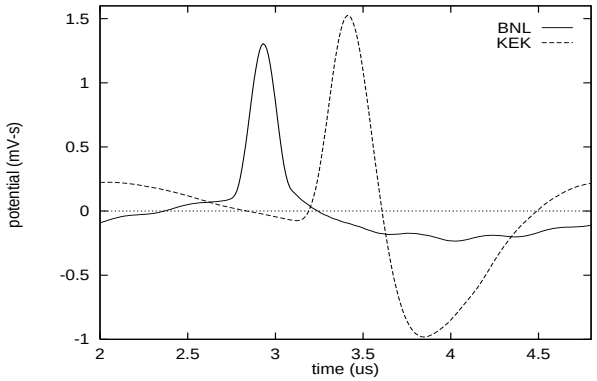

Figure 2: Integral of gap voltage without beam.

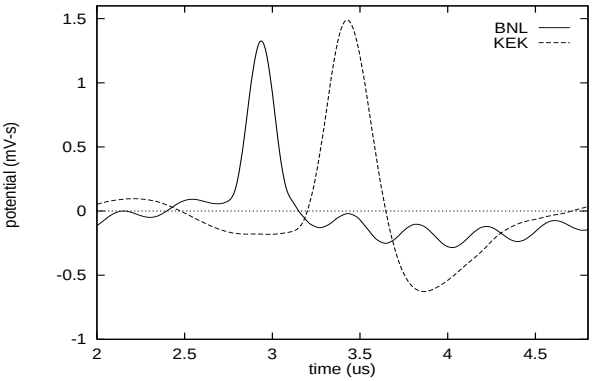

Figure 4: Integral of gap voltage with beam.

measured gap current for this cavity. The local minima in the KEK integral appear to be real.

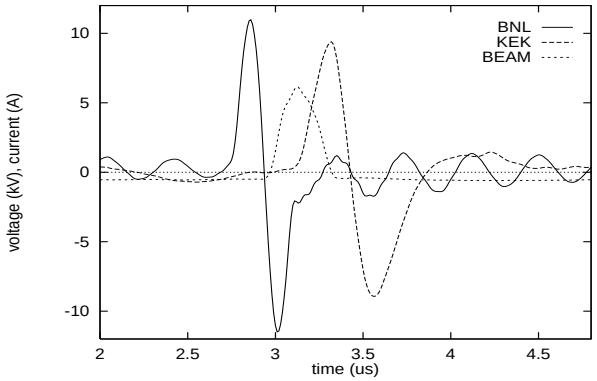

Figure 3: Gap voltage with beam and beam current. The feedforward on the KEK cavity is optimized.

Figure 3 shows the voltage waveforms of the BNL and KEK cavities along with the beam current. The oscillation in the BNL waveform is at the cavity resonant frequency with a decay rate consistent with the measured Q. The bunch contained 8.5×10^{12} protons; about the number required for the barrier cavity rf system to compete with the traditional rf system. Figure 4 shows the voltage integrals with beam.

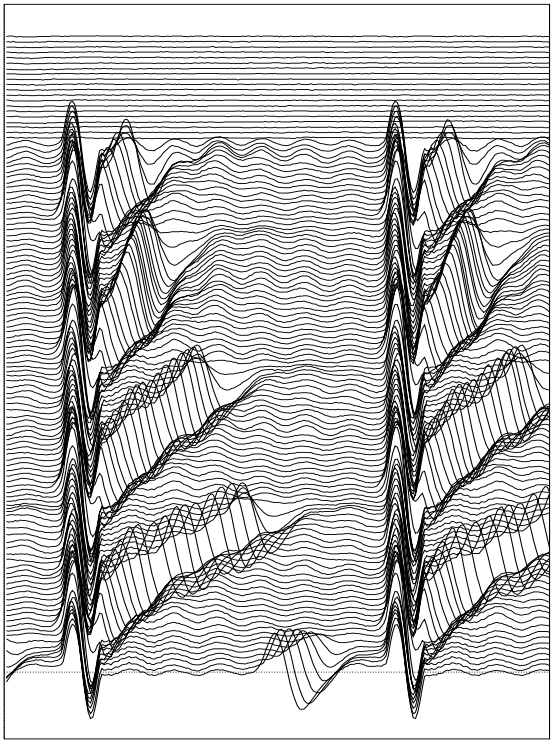

Figure 5: Mountain range plot of gap voltage for five transfers

3 MULTIPLE TRANSFERS

Controls for the barrier bucket system allowed multiple transfers, time dependent adjustment of the relative phase of the barriers, and amplitude modulation of the KEK waveform. Figure 5 shows a mountain range plot of cavity voltage used to accumulate five (5) Booster transfers. The BNL cavity was pulsed at the revolution frequency. The KEK cavity had a programmed delay and its amplitude was modulated to minimize emittance growth during coalescence. The first (bottom most) trace was taken about 100 ms after the first Booster transfer. There was 150 ms between transfers. Figure 6 shows the beam current for the same cycle as Figure 5. The ripples evident during debunching of the first transfer are due to the ripples in the BNL waveform, while the tendency for the beam to bunch toward later times is due to the asymmetry in the KEK waveform. After five transfers were accumulated the beam was rebunched slowly on $h = 6$. The final emittance was $6 \times 6.7 = 40$eV-s, 2.8 times larger than the $5 \times 2.9 = 14$eV-s emittance of the Booster beam. Simulations predict $\lesssim 10\%$ emittance growth due to rebunching and pseudo-Schottky scans were done to verify that the emittance was large before rebunching. Significant transition losses $\sim 20\%$ occurred when the beam was accelerated[4].

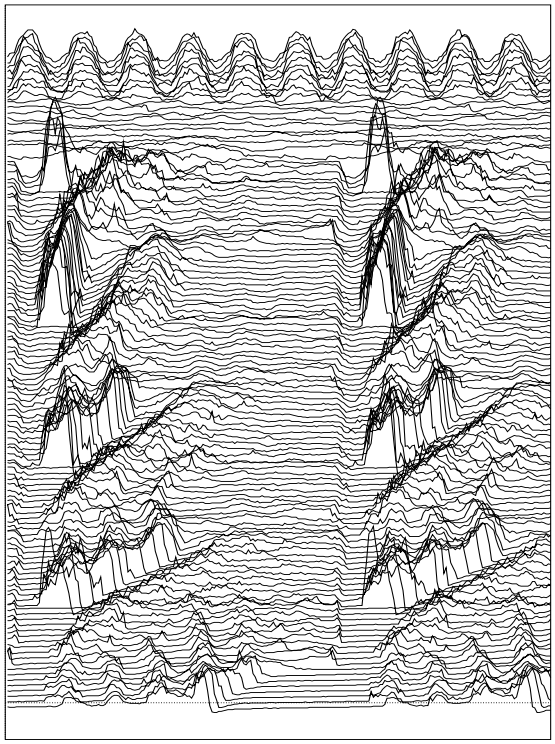

Figure 6: Mountain range plot of beam current for five transfers. A total of 3×10^{13} protons were accumulated.

4 CONCLUSIONS

The successful operation of a barrier bucket rf system appears to have several requirements. The barrier voltage pulses must closely approximate single periods of isolated sine waves. Overshoot and ripple will keep the beam from debunching or cause significant emittance growth during the process. The integral of the voltage as in Figures 2 and 4 may be more useful than the voltage itself. A well compensated voltage divider at the cavity is helpful.

Another key feature is the ability to modulate the amplitude of the barrier voltage. Rapidly turning off the waveform results in an emittance growth equal to the product of the width of the barrier and the energy spread of the stored beam.

For emittance conservation the barriers must form a matched bucket for the injected beam. This places constraints on the voltage and frequency that can be more severe than the momentum spread requirements of the debunched beam. Conversely, narrow barriers can place unacceptable constraints on the injection kicker magnet pulse, which was 800 ns in our case.

At moderate to high intensity the effects of beam loading become severe. For a low Q cavity a feedforward system is probably adequate but for high Q it is likely that some sort of feedback will be required. Since the barrier voltage is broad band there is no analogy to detuning in a harmonic rf system. To cancel the beam induced voltage the power amplifier must be able to deliver the full beam current per accelerating gap. Let $\delta I = I_b - I_f$ be the difference between the beam current and feedback/feedforward current. In a linear system $\delta I(\omega) = T(\omega) I_b(\omega)$ where T is the transfer function for voltage correction. For an RLC resonator with steady state beam loading the mean square error in the integral of the voltage is given by

$$< \delta U^2 >= 2 \left(\frac{R}{Q\omega_0} \right)^2 \sum_{n=1}^{\infty} \frac{|T(n\omega_0) I_b(n\omega_0)|^2}{(n/Q)^2 + (n^2/h - h)^2}, \quad (2)$$

where $h = \omega_r/\omega_0$ is the generalized harmonic number. The peak drive current needed to create a barrier voltage V is given by[2, 3] $I_p = V(Q+1)/R$ which, for fixed I_p and V, implies $R/Q = V(1 + 1/Q)/I_p$.

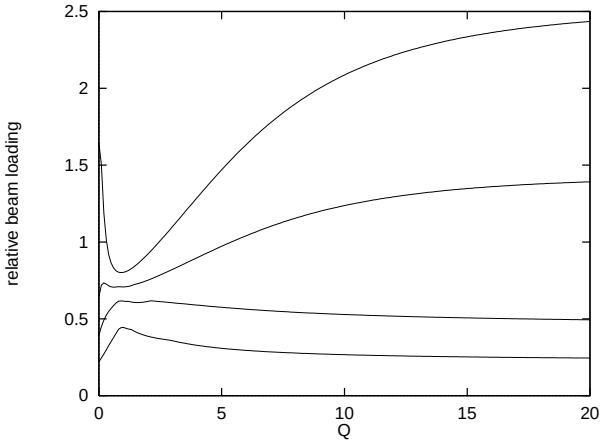

Figure 7: Sum in eq(2) with $T_n I_n = 1$ initially and then removing the largest 0,1,2, and 4 elements. The harmonic number was $h = 7.5$.

For perfect correction $T_n = 0$ while $T_n = 1$ for uncorrected lines. To illustrate the interplay of Q with feedback the elements of the sum in equation (2) were calculated with $T_n I_n = 1$, and the value of R/Q was chosen so that the voltage and peak drive current were constant. The sum using all the elements was calculated as were sums with the largest 1,2, or 4 elements set to zero. Figure 7 shows the modified sums versus Q for the four conditions. The optimal value of Q increases with the number of lines corrected.

5 ACKNOWLEDGEMENTS

We thank the members of the AGS RF group and the KEK-Tanashi RF group for their great help. The expertise and dedication of the AGS operations staff were indispensible.

6 REFERENCES

[1] J.E. Griffin, C. Ankenbrandt, J.A. MacLachlan, A. Moretti, IEEE TNS, **30**, p3502, 1983.

[2] M. Blaskiewicz, AIP conf 377 p283 (1995).

[3] M. Blaskiewicz, J.M. Brennan, EPAC96, p2373 (1996).

[4] M. Fujieda et. al. these proceedings